Surface Science 602 (2008) L127–L130

Contents lists available at ScienceDirect

Surface Science

journal homepage: www.elsevier.com/locate/susc

Surface Science Letters

Spatial modulation of the Dirac gap in epitaxial graphene

L. Vitali [a,*], C. Riedl [a], R. Ohmann [a], I. Brihuega [a], U. Starke [a], K. Kern [a,b]

[a] Max-Planck-Institut für Festkörperforschung, Heisenbergstrasse 1, D-70569 Stuttgart, Germany
[b] Institut de Physique des Nanostructures, École Polytechnique Fédéral de Lausanne, Switzerland

ARTICLE INFO

Article history:
Received 21 May 2008
Accepted for publication 16 September 2008
Available online 27 September 2008

Keywords:
Epitaxial graphene
Scanning tunneling microscopy
Scanning tunneling spectroscopy

ABSTRACT

We use scanning tunneling spectroscopy (STS) at low temperatures to investigate the local electronic structure of mono- and bilayer graphene grown epitaxially on SiC(0001). Already for monolayer graphene, a gap opening is observed in the π-bands at the Dirac point. The gap size is spatially modulated with the $(6\sqrt{3}\times 6\sqrt{3})R30^\circ$ periodicity of the interface structure. We ascribe this effect to a spatially dependent interface potential, which is imprinted into the graphene layer. For bilayer graphene the Dirac gap has a constant size, but a spatially localized mid-gap state is observed within. For both, gap state and π-bands the intensities are strongly modulated with the atomic periodicity of graphene.

Flat layers of sp^2-bonded carbon are the basic building block of graphite. As individual free-standing layers they are well-known under the name graphene. Graphene displays unconventional electronic properties [1] which make it a highly promising candidate for the realization of nano-electronic circuits [2]. In particular, monolayer graphene exhibits a linear electronic dispersion of the π-bands near the so-called Dirac point [3]. Electrons can be viewed as massless and relativistic and possess a large velocity equal to 1/300 of the speed of light. The successful preparation of single- and multilayers of graphene was first realized by mechanical exfoliation generating micron sized flakes [4,5]. For a practical application, however, the ability to prepare graphene on a large scale and supported on a substrate would be of advantage. Besides first successful approaches based on the reduction of graphene oxide [6], the epitaxial growth of graphene on hexagonal SiC surfaces by thermal decomposition of the topmost SiC bilayers of the substrate is very promising in this respect [7]. On SiC(0001), mono- and few-layer graphene can be successfully grown in a controlled manner [7–10]. The number of graphene layers grown in this fashion determines the splitting into different branches of the π-bands crossing the Dirac point [11,12].

For a slab of two layers of graphene, the opening of a gap at the Dirac point is expected [11] and indeed found experimentally [12,13]. Yet, the exact size of the gap, its position in the energy diagram, and in particular whether this gap opens also for a single graphene layer, are currently disputed. Using angle-resolved photoemission spectroscopy (ARPES) Bostwick et al. found that no gap exists for monolayer graphene [14], while in a different experiment with the same method a gap was discovered already for the first graphene layer [13]. It is important to understand the electronic structure and possible presence of a gap in this regime for epitaxial graphene since it has an important impact on potential applications such as field effect devices. In the present paper we use scanning tunneling spectroscopy (STS) to investigate the electronic structure of epitaxial graphene with high spatial resolution and demonstrate the presence of a gap already for monolayer graphene.

According to theoretical predictions, the opening of a gap in the π-band dispersion can be caused by different effects. Symmetry breaking within the graphene layers affects the band structure and induces a gap in the local density of states (LDOS) at the Dirac energy [15,16]. In particular, an interlayer stacking sequence such as, for instance, Bernal AB stacking, leads to a non-equivalency of the two carbon atoms in the graphene unit cell. This type of symmetry breaking within the graphene unit cell induced by the substrate-graphene stacking was suggested to explain the gap observed in the monolayer [13]. An additional symmetry breaking in epitaxial graphene can originate from a charge transfer between the first graphene layers and the substrate. The charge accumulation at the interface creates a dipole potential, whereby the effect is reduced by screening in additionally grown layers. As a consequence the first few layers of epitaxial graphene are not equivalent with respect to charge and electrostatic potential. The sensitivity of the electronic structure in graphene to such an electrostatic potential has been demonstrated by the successful control of the gap size by depositing electron-donor impurities (K atoms) on the graphene surface [9].

The lattice mismatch between graphene and the SiC substrate gives rise to a complex atomic structure of the interface in epitaxial

* Corresponding author. Tel.: +49 711 6891538; fax: +49 711 6891662.
E-mail address: l.vitali@fkf.mpg.de (L. Vitali).

0039-6028/$ - see front matter © 2008 Elsevier B.V. All rights reserved.
doi:10.1016/j.susc.2008.09.030

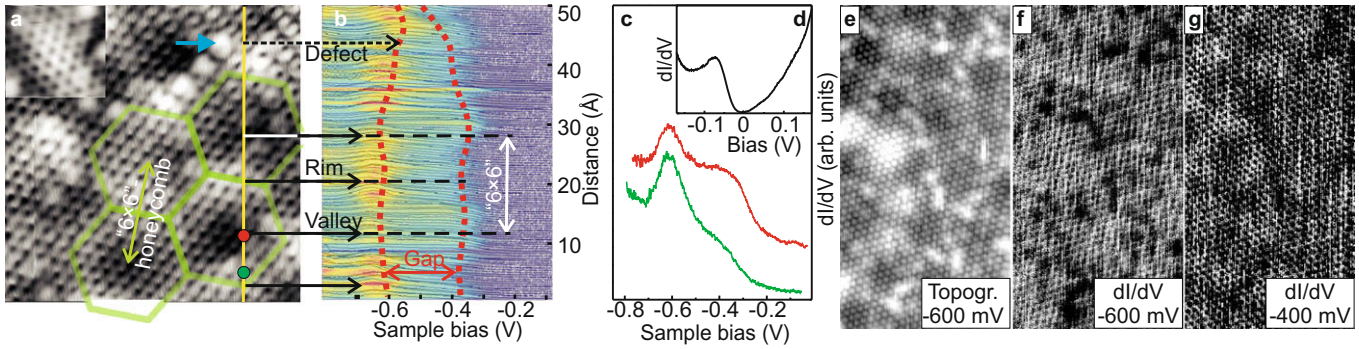

Fig. 1. Monolayer graphene: (a) Topographic region (image size 50 Å × 50 Å, sample bias 100 mV, 0.5 nA, inset at 440 mV). The green hexagons indicate the quasi-"(6 × 6)" periodicity. (b) Color scale plot of d*I*/d*V* spectra obtained along the yellow line in (a). The dashed lines mark the positions of the π-band onsets as a guide to the eye. (c) Selected d*I*/d*V* spectra obtained on the positions marked with a dot in (a) displayed with a vertical shift for better visualization. (d) d*I*/d*V* Spectrum at the Fermi energy. (e–g) Topographic image and conductance maps (image size 100 Å × 50 Å) simultaneously measured at the energy of the π-band onset. (For interpretation of the references to colour in this figure legend, the reader is referred to the web version of this article.)

graphene. This is quite obvious from its large commensurate unit cell with a $(6\sqrt{3} \times 6\sqrt{3})R30^\circ$ periodicity as seen in low-energy electron diffraction (LEED) [10,17,18]. The interface is formed by the first carbon layer evolving in the annealing process, which does not yet possess a linear π-band dispersion at the Dirac point and rather acts like a buffer layer [19]. Only the next carbon layer has typical graphene properties and corresponds to a graphene monolayer. Further heating then leads to bilayer graphene. The nature of the interfacial buffer layer must have a significant electronic influence on the subsequent layers, since it has a strong and bias dependent electronic corrugation as seen in scanning tunneling microscopy (STM). Under most conditions it is imaged as a quasi-"(6 × 6)" pattern characterized by a honeycomb or hillock structure [20,21]. Only at certain bias values its true $(6\sqrt{3} \times 6\sqrt{3})R30^\circ$ periodicity is observed [10]. The aim of the present work is to investigate the influence of this spatially strongly modulated electronic structure on the dispersion of the π-bands in the epitaxial graphene layers. For this purpose we measure the LDOS of graphene grown on SiC with high spatial resolution using STS at low temperatures.

Samples, cut from a 4H-SiC(0001) wafer,[1] were hydrogen etched for the removal of polishing damage [22]. In order to enable a homogeneous graphene growth [10], Si deposition and annealing steps were taken in ultra-high vacuum (UHV), first to the Si-rich (3 × 3) phase [23] and then to a well-ordered $(\sqrt{3} \times \sqrt{3})R30^\circ$ Si adatom reconstruction [24]. The $(6\sqrt{3} \times 6\sqrt{3})R30^\circ$ periodic buffer layer was obtained by annealing to temperatures above 1150 °C [10]. Graphene layers were then generated by annealing at even higher temperature. Their thickness was characterized by LEED [10,28]. The prepared graphene sample was then transferred ex situ to the STM chamber. In UHV the sample was again annealed up to 1050 K in order to desorb impurities. The topographic and spectroscopic measurements were conducted with a UHV–STM at a temperature of ≈6 K.

An STM topographic image of a graphene monolayer is shown in Fig. 1a. It shows the graphene structure superimposed onto the periodicity of the underlying buffer layer in agreement with previous reports [10,25–27]. The structure of the buffer layer can be seen through the graphene grid as a honeycomb shaped wall structure as indicated by the green hexagons. The typical terrace width is at least 200 Å. In panel c, d*I*/d*V* spectra are shown for the positions marked with dots in panel a. All spectra exhibit two peaks at energies close to the Dirac point, which can be attributed to the onsets of the π-bands. This indicates that the π-bands are separated by an energy gap. The Dirac point as determined by the median of the two band onsets is shifted with respect to the Fermi level (E_F) by about −460 MV, which is in agreement with reported [12,13] and home laboratory ARPES measurements [28]. The observation of a gap opening for monolayer graphene is in contrast to Ohta et al. [9] but in accordance with Zhou et al. [13]. However, the gap can not simply be due to an AB asymmetry of the two atoms per unit cell caused by a Bernal-type stacking with respect to the buffer layer [25,26,29] as all six atoms of the hexagonal honeycomb of graphene are retrieved (inset in panel a).

Most importantly, our STM measurements reveal that the peak positions vary in energy according to the periodicity of the interface structure. The modulation of the Dirac gap is visualized in Fig. 1b. It shows in a color scale map the d*I*/d*V* spectra measured along the yellow line marked in panel a.[2] The positions of the π-band onsets (red dashed lines) vary smoothly and fluctuate with the quasi-"(6 × 6)" periodicity (green hexagons) of the buffer layer. The average value of the gap is 220 mV with a modulation around the Dirac energy of about ±40 mV between valley (maximum) and rim (minimum) positions. Still, the Dirac energy remains constant except in close proximity to defects (blue arrow in Fig. 1a) [26,30]. Here, also the gap is significantly reduced. For completeness also the d*I*/d*V* spectrum at the Fermi energy on the monolayer is shown in panel d. The observed line shape demonstrates the (still not understood) electronic DOS of epitaxial graphene, previously reported [25,27].

In order to understand the possible origin of the spatially modulated Dirac gap, energy resolved conductance maps at the π-band onsets were obtained by recording the d*I*/d*V* signal at the corresponding bias values (see Fig. 1). Together with a topographic map (panel e), they are shown in panel f and g. The impact of the buffer layer structure on the graphene monolayer is evident. At −400 mV a modulating potential with a quasi-"(6 × 6)" periodicity is superimposed onto the structure of the graphene monolayer (panel g). At −600 mV dark dots (points of lower conductance) can be seen (panel f). The absence of electronic scattering around them excludes their origin to be from adsorbed impurities on the graphene layer. At the first glance these dots do not seem to form an ordered pattern. However, by superimposing the topographic image onto the conductance map the dots can be correlated with the bright atom-like features in the quasi-"(6 × 6)" honeycomb pattern of the buffer layer. This suggests that

[1] Resistivity: 0.017 Ω cm, n-type, N doped.

[2] The d*I*/d*V* spectra and the energy resolved conductance maps reported in this letter have been recorded by means of a lock-in technique applying a sample bias modulation in the range of 10–15 mV.

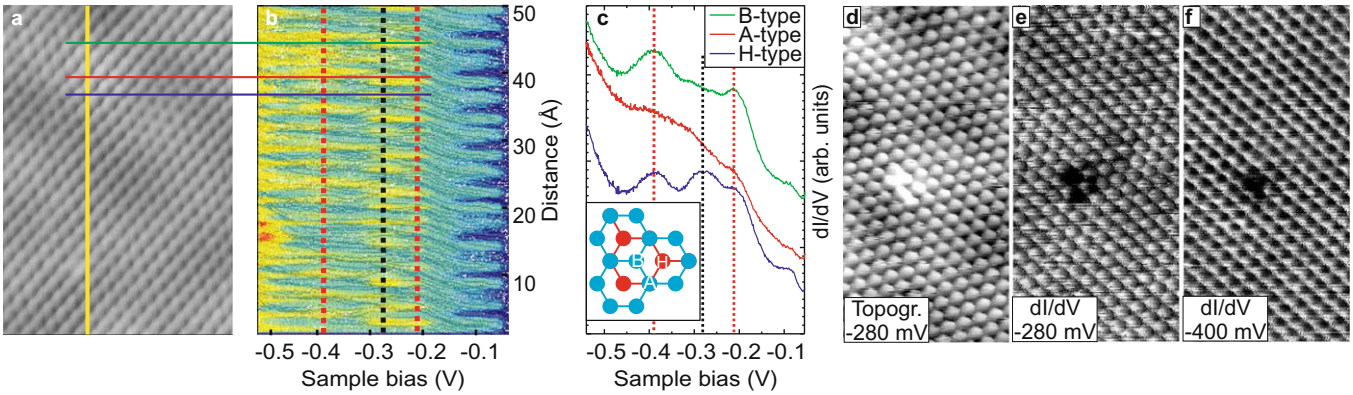

Fig. 2. Bilayer graphene: (a) Topographic region (image size 50 Å × 35 Å, sample bias −400 mV, 0.5 nA). (b) Color scale plot of d*I*/d*V* spectra obtained along the yellow line in (a). The dashed lines indicate the positions (red) of the π-band onsets and the mid-gap state (black). Horizontal lines correlate the three high symmetry positions in the graphene unit cell with typical spectra displayed with a vertical shift in (c). The inset shows a sketch of the graphene bilayer stacking. (d–f) Topographic image and conductance maps simultaneously measured at −280 and −400 mV, respectively (image size 50 Å × 25 Å). (For interpretation of the references to colour in this figure legend, the reader is referred to the web version of this article.)

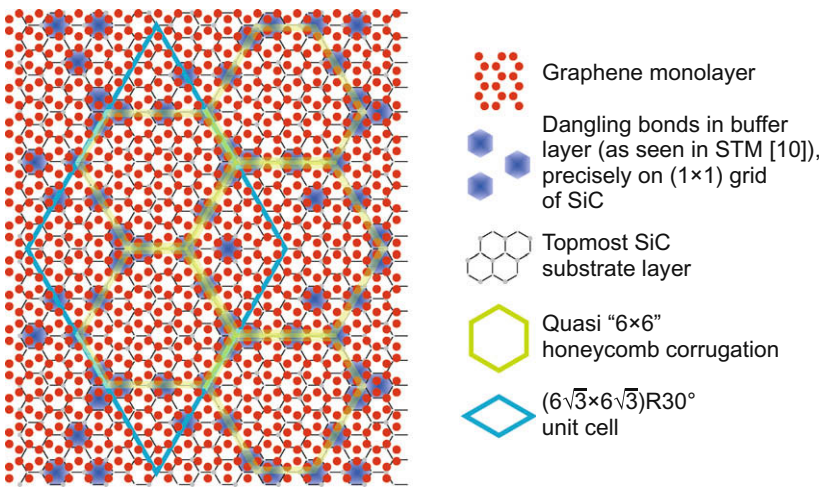

Fig. 3. Tentative sketch of the positions of carbon atoms (red dots) in the epitaxial graphene monolayer. The position of bright spots observed in STM on the buffer layer [10] are indicated by the shaded blue hexagons. Green hexagons and the blue diamond indicate the quasi-"(6 × 6)" honeycomb and the $(6\sqrt{3} \times 6\sqrt{3})R30^\circ$ unit cell observed on the buffer layer [10]. (For interpretation of the references to colour in this figure legend, the reader is referred to the web version of this article.)

different atoms of the graphene monolayer are electronically distinct due to the structure of the buffer layer.

For bilayer graphene, the topographic image (Fig. 2a) contains much less contributions from the interface (see also [30]). The LDOS was evaluated along the yellow line. In the d*I*/d*V* map (panel b) and the averaged spectra (panel c, see below) a gap around the Dirac point is clearly visible in agreement with previous ARPES work [9,13]. The gap, of about 180 mV, is centered around 300 mV below E_F. As indicated by the dashed red lines, in this case the peaks do not vary in energy along the measured line. Instead, the π-band varies substantially in intensity with the atomic graphene periodicity. Also a localized mid-gap state appears in strict correlation with the atom position in the graphene unit cell. For the three different high symmetry positions in the unit cell, averaged spectra are shown in panel c. At the position of the B-type atoms, which corresponds to the bright spots in the topographic image [29], only the π-band onsets are seen. On one of the dark areas aside of a B-type atom these states are attenuated while on the other side an additional peak at −280 mV appears. This mid-gap state is localized on one of the hollow site positions, as can be seen also in the conductance map (panel e) achieved simultaneously to the topographic image (panel d). Since a mid-gap state is, in flat free-standing graphene, not predicted nor experimentally observed, we can tentatively assign it to a tip induced state. Similar to graphite, the influence of the tip on graphene multilayers can distort the interlayer distance [31,32]. As a curvature of the graphene layer is theoretically predicted to induce the formation of a mid-gap state [33], we speculate that the tip-induced layer distortion is the origin of the observed mid-gap state [31,32]. The tip interaction is predicted to be stronger on the H-type atom at our tip-sample distance, which can be estimated to be 5 Å. Accordingly, we assigned the observed mid-gap state to the H-type position (blue curve in panel c). We note that also the conductance maps show no modulation with the periodicity of the buffer layer (panels e and f).

To better elucidate the role of the buffer layer on the graphene monolayer we sketch in a tentative model (Fig. 3) the registry relation between the different layers. As shown recently by STM [10], on the pure buffer layer a number of dangling-bond like features (bright spots in STM) are distributed along the walls of the "(6 × 6)"-honeycomb (green hexagons in the figure, of slightly varying size due to the true $(6\sqrt{3} \times 6\sqrt{3})R30^\circ$ periodicity). As indi-

cated by shaded blue areas, they are situated exactly on (1×1) SiC-substrate grid positions. Consequently, in the superimposed graphene layer the different C atoms (red dots) within the $(6\sqrt{3} \times 6\sqrt{3})R30^\circ$ unit cell are not equivalent with respect to the coupling to the buffer layer. Thus, a spatially dependent electronic influence of the buffer layer must be expected. We assign the gap separating the π-bands to this effect. It is worth noting that this influence originates from the quasi-"(6×6)" corrugation of the interface potential and not from a stacking induced symmetry breaking within the unit cell as proposed by Zhou et al. [13]. Our results rather support the scenario that a gap opens due to a super-periodicity as suggested by Mañes et al. [34]. This scenario is in agreement with recent ARPES measurements on the buffer layer and graphene monolayer [35]. These measurements indicate the presence of two localized states on the buffer layer. These shift, respectively to higher or lower energies with respect to the peaks discussed in this work when the graphene monolayer is grown. This allows us to exclude that the observed electronic structure derives from the interface layer. In contrast to the monolayer case, for a bilayer the gap size is constant and the conductance maps show mainly a graphene structure which is only weakly perturbed by the buffer layer periodicity. Apparently, the buffer layer potential is screened by the first graphene layer and has essentially no influence on the LDOS. However, in bilayer graphene the states are modulated by the atomic periodicity of graphene.

In conclusion our experimental data reveal the presence of a spatially modulated and thickness dependent gap at the Dirac energy in epitaxial graphene. For monolayer graphene, the gap size is strongly modulated with the buffer layer periodicity which we attribute to the influence by a spatially varying potential of the interface. The mechanism of the gap opening must be connected to the super-periodicity of the interface rather than a symmetry breaking within the graphene unit cell as previously suggested [13]. Quite differently, in bilayer graphene the gap size is constant, but the π-bands display a strong localization with the graphene periodicity itself. The additional appearance of a localized state within the gap may be correlated to a tip induced local distortion of the graphene layers.

Acknowledgement

We acknowledge L. Boeri for the fruitful discussion. I.B. was supported by the European Community as part of a Marie Curie host fellowship.

References

[1] P.R. Wallace, Phys. Rev. 71 (1947) 622.
[2] A.K. Geim, K.S. Novoselov, Nat. Mater. 6 (2007) 183.
[3] D.P. DiVincenzo, E.J. Mele, Phys. Rev. B 29 (1984) 1685.
[4] K.S. Novoselov et al., Science 306 (2004) 666.
[5] K.S. Novoselov et al., Nature 438 (2005) 197.
[6] C. Gómez-Navarro et al., Nanoletters 7 (2007) 3499.
[7] C. Berger et al., J. Phys. Chem. B 108 (2004) 19912.
[8] C. Berger et al., Science 312 (2006) 1191.
[9] T. Ohta et al., Science 313 (2006) 951.
[10] C. Riedl et al., Phys. Rev. B 76 (2007) 245406.
[11] B. Partoens, F.M. Peeters, Phys. Rev. B 74 (2006) 075404.
[12] T. Ohta et al., Phys. Rev. Lett. 98 (2007) 206802.
[13] S.Y. Zhou et al., Nat. Mater. 6 (2007) 770.
[14] A. Bostwick et al., Nat. Phys. 3 (2007) 36.
[15] E. McCann, Phys. Status Solidi 244 (2007) 4112.
[16] N.M.R. Peres, F. Guinea, A.H. Castro Neto, Phys. Rev. B 73 (2006) 125411.
[17] A.J. van Bommel, J.E. Crombeen, A. van Tooren, Surf. Sci. 48 (1975) 463.
[18] I. Forbeaux, J.-M. Themlin, J.M. Debever, Phys. Rev. B 58 (1998) 16396.
[19] K.V. Emtsev et al., Mater. Sci. Forum 556–557 (2007) 525.
[20] P. Mårtensson, F. Owman, L.I. Johansson, Phys. Status Solidi (b) 202 (1997) 501.
[21] W. Chen et al., Surf. Sci. 596 (2005) 176.
[22] S. Soubatch et al., Mater. Sci. Forum 483–485 (2005) 761.
[23] U. Starke et al., Phys. Rev. Lett. 80 (1998) 758.
[24] U. Starke et al., Phys. Rev. Lett. 82 (1999) 2107.
[25] W.V. Brar et al., Appl. Phys. Lett. 91 (2007) 122102.
[26] P. Mallet et al., Phys. Rev. B 76 (2007) 041403(R).
[27] G.M. Rutter et al., Phys. Rev. B 76 (2007) 235416.
[28] C. Riedl, A.A. Zakharov, U. Starke, Appl. Phys. Lett. 93 (2008) 033106.
[29] D. Tománek et al., Phys. Rev. B 35 (1987) 7790.
[30] G.M. Rutter et al., Science 317 (2007) 219.
[31] J.M. Soler, A.M. Baro, N. Garcia, H. Rohrer, Phys. Rev. Lett. 57 (1986) 444.
[32] S. Ciraci, I.P. Batra, Phys. Rev. B 36 (1987) 6194.
[33] F. Guinea, M.I. Katsnelson, M.A.H. Vozmediano, Phys. Rev. B 77 (2008) 075422.
[34] J.L. Mañes, F. Guinea, M.A.H. Vozmediano, Phys. Rev. B 75 (2007) 155424.
[35] K.V. Emtsev et al., Phys. Rev. B 757 (2008) 155303.